Parametric Methods for Power Spectral Density Estimation

Reza Moosavi

As discussed earlier, we would like to estimate the power spectral density (PSD) of the signal $y(t)$, which is obtained by filtering white noise $e(t)$ of power σ^2 through the rational stable and causal filter with the transfer function $H(\omega) = B(\omega)/A(\omega)$, where

$$A(\omega) = 1 + a_1 e^{-i\omega} + \ldots + a_n e^{-in\omega}$$
$$B(\omega) = 1 + b_1 e^{-i\omega} + \ldots + b_m e^{-im\omega}.$$

In the time domain, the above filtering can be represented as

$$y(t) + \sum_{i=1}^{n} a_i y(t-i) = \sum_{j=0}^{m} b_j e(t-j), \quad (b_0 = 1). \tag{1}$$

We further divide this problem intro three categories based on the values of m and n:

- (i) If both m and n are non-zero, then the signal is said to be *Auto-regressive moving average* (ARMA) and is denoted by ARMA(n, m).
- (ii) If $m = 0$, then the signal is an *auto-regressive* (AR) signal and is denoted by AR(n); and finally,
- (iii) If $n = 0$, the signal is a *moving average* (MA) signal and is denoted by MA(m).

I. Covariance Structure of ARMA Processes

In this section, we provide an expression for the covariance of a general ARMA process. Multiplying both sides in (1) by $y^*(t-k)$ and taking expectation yields

$$r(k) + \sum_{i=1}^{n} a_i r(k-i) = \sum_{j=0}^{m} b_j E\left\{e(t-j)y^*(t-k)\right\}. \tag{2}$$

To simplify (2) further, we use the fact that $H(q) = B(q)/A(q)$ is causal and stable, that is, we can write

$$H(q) = \frac{B(q)}{A(q)} = \sum_{\ell=0}^{\infty} h_\ell q^{-\ell}, \quad (h_0 = 1)$$

and thus

$$y(t) = H(q)e(t) = \sum_{\ell=0}^{\infty} h_\ell e(t-\ell).$$

Therefore, the term $E\{e(t-j)y^*(t-k)\}$ becomes

$$\begin{aligned} E\{e(t-j)y^*(t-k)\} &= E\left\{e(t-j)\sum_{\ell=0}^{\infty} h_\ell^* e^*(t-k-\ell)\right\} \\ &= \sigma^2 \sum_{\ell=0}^{\infty} h_\ell^* \delta_{j,k+\ell} = \sigma^2 h_{j-k}^*. \end{aligned} \tag{3}$$

Substituting (3) into (2), we get

$$r(k) + \sum_{i=1}^{n} a_i r(k-i) = \sigma^2 \sum_{j=0}^{m} b_j h_{j-k}^*. \tag{4}$$

Note that since $H(q)$ is causal, $h_\ell = 0$ for $\ell < 0$. This means that for $k \geq m+1$, equation (4) can be further simplified to

$$r(k) + \sum_{i=1}^{n} a_i r(k-i) = 0, \quad \text{for} \quad k > m. \tag{5}$$

This equation plays an important rule for many estimation techniques, as we will see.

II. AR Signals: Yule-Walker Method

In this section, we derive the so-called *Yule-Walker method* for estimating the PSD of AR signals. For AR signals, $m = 0$ and $B(q) = 1$. From equation (4) we have

$$r(0) + \sum_{i=1}^{n} a_i r(-i) = \sigma^2 \sum_{j=0}^{0} b_j h_{j-k}^* = \sigma^2 \tag{6}$$

for $k = 0$. Also for $k = 1, \ldots, n$, we can use (5) repeatedly. Combining these two and representing the result in a matrix form, we have the following system of linear equations

$$\begin{bmatrix} r(0) & r(-1) & \ldots & r(-n) \\ r(1) & r(0) & \ldots & r(-n+1) \\ \vdots & \vdots & \ddots & \vdots \\ r(n) & r(n-1) & \ldots & r(0) \end{bmatrix} \begin{bmatrix} 1 \\ a_1 \\ \vdots \\ a_n \end{bmatrix} = \begin{bmatrix} \sigma^2 \\ 0 \\ \vdots \\ 0 \end{bmatrix} \tag{7}$$

The above equations are called the Yule-Walker or Normal equations. If $\{r(k)\}_{k=0}^{n}$ were known, we could use all but the first row of (7) to find the coefficients $a_1, \ldots, a_n$ and substituting the resulting coefficients into the first row to find σ^2. More precisely, we have

$$\underbrace{\begin{bmatrix} r(1) \\ \vdots \\ r(n) \end{bmatrix}}_{\triangleq \boldsymbol{r}_n} + \underbrace{\begin{bmatrix} r(0) & \ldots & r(-n+1) \\ \vdots & \ddots & \vdots \\ r(n-1) & \ldots & r(0) \end{bmatrix}}_{\triangleq R_n} \underbrace{\begin{bmatrix} a_1 \\ \vdots \\ a_n \end{bmatrix}}_{\triangleq \boldsymbol{\theta}} = \begin{bmatrix} 0 \\ \vdots \\ 0 \end{bmatrix} \tag{8}$$

and thus $\boldsymbol{\theta} = -R_n^{-1}\boldsymbol{r}_n$ and once $\boldsymbol{\theta}$ is found, σ^2 can be found by using the first row of (7).

The Yule-Walker method for estimating the spectrum of an AR signal is based on the above Yule-Walker equations. More precisely, we first obtain sample covariances $\{\hat{r}(k)\}_{k=0}^{n}$ from the observed sequence, using the standard biased estimator

$$\hat{r}(k) = \frac{1}{N} \sum_{t=k+1}^{N} y(t) y^*(t-k), \quad 0 \leq k \leq N-1 \tag{9}$$

and then, we use (7) and (8) to obtain θ and σ^2 respectively.

III. Order-Recursive Solutions to the Yule-Walker Equations

In applications, where the degree n of the AR process is known a priori, then the Yule-Walker method can be used to find the spectrum of the signal. However, when the degree of the AR process in not known beforehand, the spectrum of the signal is computed for different but predefined values of n. That is, the spectral is estimated assuming all values of $n \in \{1, 2, \ldots, n_{\max}\}$ and the "best" estimate is chosen according to some criteria as the ultimate spectral estimator. Since $n_{\max}$ is large in some applications, the computational complexity of

doing so can be unacceptably high. More precisely, the computational complexity is

$$\sum_{n=1}^{n_{\max}} \mathcal{O}(n^3) = \mathcal{O}(n_{\max}^4),$$

where we assume that the computational complexity of the Yule-Walker method for obtaining the spectrum of an AR(n) process is $\mathcal{O}(n^3)$ due to the requirement for inversion of the $n \times n$ matrix R_n in (8).

Many algorithms have been proposed to reduce the complexity in such scenarios. In this section, we introduce the *Levinson-Durbin algorithm* (LDA), which uses the specific structure of the covariance matrices R_n to compute the AR parameters recursively. Before that, we need the following preliminaries.

First, to explicitly show the dependence of the AR parameters to the AR degree n, we write (7) as

$$R_{n+1} \begin{bmatrix} 1 \\ \boldsymbol{\theta}_n \end{bmatrix} = \begin{bmatrix} \sigma_n^2 \\ \mathbf{0} \end{bmatrix}. \tag{10}$$

Let ρ_k denote $r(k)$ (or $\hat{r}(k)$ when the sample covariances are used). Since $r(-k) = r^*(k)$, we have

$$R_{n+1} = \begin{bmatrix} \rho_0 & \rho_{-1} & \cdots & \rho_{-n} \\ \rho_1 & \rho_0 & \cdots & \rho_{-n+1} \\ \vdots & \vdots & \ddots & \vdots \\ \rho_n & \rho_{n-1} & \cdots & \rho_0 \end{bmatrix} = \begin{bmatrix} \rho_0 & \rho_1^* & \cdots & \rho_n^* \\ \rho_1 & \rho_0 & \cdots & \rho_{n-1}^* \\ \vdots & \vdots & \ddots & \vdots \\ \rho_n & \rho_{n-1} & \cdots & \rho_0 \end{bmatrix} \tag{11}$$

and thus R_{n+1} is Hermitian. Also we can see that R_{n+1} is Toeplitz. This enables us to use an important property for Hermitian Toeplitz matrix R, namely

$$\boldsymbol{y} = R\boldsymbol{x} \quad \Rightarrow \tilde{\boldsymbol{y}} = R\tilde{\boldsymbol{x}}, \tag{12}$$

where for a vector $\boldsymbol{x} = [x_1 \dots x_n]$, we define $\tilde{\boldsymbol{x}} \triangleq [x_n^* \dots x_1^*]$. This result follows readily from the following calculation:

$$\begin{aligned} \tilde{y}_i = y_{n-i+1}^* &= \left((R\boldsymbol{x})_{n-i+1}\right)^* = \sum_{k=1}^{n} R_{n-i+1,k}^* x_k^* \\ &= \sum_{k=1}^{n} \rho_{n-i+1-k}^* x_k^* = \sum_{k=1}^{n} \rho_{i-k} x_{n-k+1}^* = (R\tilde{\boldsymbol{x}})_i \end{aligned}$$

IV. LEVINSON-DURBIN ALGORITHM

The basic idea of LDA is to solve (10) recursively in n, starting from the trivial solution for $n = 1$:

$$\theta_1 = -\frac{\rho_1}{\rho_0}, \qquad \sigma_1^2 = \rho_0 - \frac{|\rho_1|^2}{\rho_0}$$

Now assume that the solution at stage n is known. Using this known solution, we would like to find the solution at stage $n+1$. In other words, knowing $\boldsymbol{\theta}_n$ and σ_n^2 from (10), we would like to solve

$$R_{n+2} \begin{bmatrix} 1 \\ \boldsymbol{\theta}_{n+1} \end{bmatrix} = \begin{bmatrix} \sigma_{n+1}^2 \\ \mathbf{0} \end{bmatrix}.$$

for $\boldsymbol{\theta}_{n+1}$ and σ_{n+1}^2. In order to do so, we use the nested structure of R_{n+2}. First note that

$$R_{n+2} = \left[\begin{array}{cccc|c} \rho_0 & \rho_{-1} & \cdots & \rho_{-n} & \rho_{-n-1} \\ \rho_1 & \rho_0 & \cdots & \rho_{-n+1} & \rho_{-n} \\ \vdots & \vdots & \ddots & \vdots & \vdots \\ \rho_n & \rho_{n-1} & \cdots & \rho_0 & \rho_{-1} \\ \hline \rho_{n+1} & \rho_n & \cdots & \rho_1 & \rho_0 \end{array}\right] = \left[\begin{array}{cccc|c} \rho_0 & \rho_1^* & \cdots & \rho_n^* & \rho_{n+1}^* \\ \rho_1 & \rho_0 & \cdots & \rho_{n-1}^* & \rho_n^* \\ \vdots & \vdots & \ddots & \vdots & \vdots \\ \rho_n & \rho_{n-1} & \cdots & \rho_0 & \rho_1^* \\ \hline \rho_{n+1} & \rho_n & \cdots & \rho_1 & \rho_0 \end{array}\right]$$

$$= \left[\begin{array}{cc|c} \multicolumn{2}{c|}{R_{n+1}} & \begin{matrix} \rho_{n+1}^* \\ \tilde{\boldsymbol{r}}_n \end{matrix} \\ \hline \rho_{n+1} & \tilde{\boldsymbol{r}}_n^* & \rho_0 \end{array}\right]$$

where $\boldsymbol{r}_n = [\rho_1 \dots \rho_n]^T$. Multiplying R_{n+2} with the vector $\boldsymbol{s}_n \triangleq [1 \ \boldsymbol{\theta}_n \ 0]^T$ and using the fact that

$$\left[\begin{array}{c|c} A & B \\ \hline C & D \end{array}\right] \left[\begin{array}{c} \boldsymbol{x}_1 \\ \hline \boldsymbol{x}_2 \end{array}\right] = \left[\begin{array}{c} A\boldsymbol{x}_1 + B\boldsymbol{x}_2 \\ \hline C\boldsymbol{x}_1 + D\boldsymbol{x}_2 \end{array}\right]$$

we can write

$$R_{n+2}\boldsymbol{s}_n = \left[\begin{array}{cc|c} \multicolumn{2}{c|}{R_{n+1}} & \begin{matrix} \rho_{n+1}^* \\ \tilde{\boldsymbol{r}}_n \end{matrix} \\ \hline \rho_{n+1} & \tilde{\boldsymbol{r}}_n^* & \rho_0 \end{array}\right] \left[\begin{array}{c} 1 \\ \boldsymbol{\theta}_n \\ \hline 0 \end{array}\right] = \left[\begin{array}{c} \sigma_n^2 \\ \mathbf{0} \\ \hline \alpha_n \end{array}\right] \tag{13}$$

where $\alpha_n = \rho_{n+1} + \tilde{\boldsymbol{r}}_n^* \boldsymbol{\theta}_n$. As we see, if α_n were zero, then (13) would be the counterpart of

(10) when n is increased by one. To make that happen, we define $k_{n+1} = -\alpha_n/\sigma_n^2$. Now using the fundamental result for Hermitian Toeplitz matrices given in (12), we see that

$$R_{n+2}\left(s_n + k_{n+1}\tilde{s}_n\right) = \begin{bmatrix} \sigma_n^2 \\ \mathbf{0} \\ \alpha_n \end{bmatrix} + k_{n+1}\begin{bmatrix} \alpha_n^* \\ \mathbf{0} \\ \sigma_n^2 \end{bmatrix} = \begin{bmatrix} \sigma_n^2 + k_{n+1}\alpha_n^* \\ \mathbf{0} \end{bmatrix}. \tag{14}$$

Therefore, by comparing (14) with

$$R_{n+2}\begin{bmatrix} 1 \\ \boldsymbol{\theta}_{n+1} \end{bmatrix} = \begin{bmatrix} \sigma_{n+1}^2 \\ \mathbf{0} \end{bmatrix}. \tag{15}$$

we reach to the conclusion that,

$$\boldsymbol{\theta}_{n+1} = \begin{bmatrix} \boldsymbol{\theta}_n \\ 0 \end{bmatrix} + k_{n+1}\begin{bmatrix} \tilde{\boldsymbol{\theta}}_n \\ 1 \end{bmatrix} \tag{16}$$

and

$$\sigma_{n+1}^2 = \sigma_n^2\left(1 - |k_{n+1}|^2\right) \tag{17}$$

The computational complexity of finding the solution at stage n is $\mathcal{O}(n)$, due to the matrix multiplication required for computation of α_n. Hence, the total computational complexity of LDA algorithm can be written as

$$\sum_{n=1}^{n_{\max}} \mathcal{O}(n) = \mathcal{O}(n_{\max}^2).$$

Thus LDA algorithm can decrease the computational complexity of finding the spectrum by two orders of magnitude.

V. MA SIGNALS

Based on the definition, an MA signal is obtained by filtering white noise through an *all-zero* filter. Due to lack of poles in the corresponding filter transfer function, the MA model cannot represent the spectrum with narrow peaks well, unless the degree is chosen sufficiently large. This puts somehow a heavy restriction on the use of MA model for engineering applications, since most of the time we are interested in estimating the spectrum that has narrow peaks. In this section, we will introduce a method for spectral estimation using MA model. We first note

that for MA signals, we have

$$y(t) = \sum_{j=0}^{m} b_j e(t-j)$$

and hence

$$r(k) = 0, \qquad \text{for } k > m.$$

Since the covariance function $r(k)$ consists of finite number of lags, the power spectral density of an MA signal also includes finite number of components and is given by

$$\phi(\omega) = \sum_{k=-m}^{m} r(k) e^{-ik\omega}. \tag{18}$$

Hence a simple estimate of the PSD is given by inserting sample covariances $\{\hat{r}(k)\}_{k=0}^{m}$ into (18), resulting in

$$\hat{\phi}(\omega) = \sum_{k=-m}^{m} \hat{r}(k) e^{-ik\omega}. \tag{19}$$

This estimator has exactly the same form as that of the Blackman-Tukey estimator with a rectangular window of length $2m+1$, see nonparametric methods for spectral estimation. Since the Blackman-Tukey estimator has been covered in the previous lecture, we leave the details to the readers.

VI. ARMA Signals

Spectra with both narrow peaks and flat nulls cannot be represented with only the AR model or the MA model (at least with the finite length). There are also other examples where modeling according to only AR or MA models fails to represent the spectra well. In those situations, the ARMA model is a good alternative. There is a computational problem with the ARMA model though, namely finding the optimum filter coefficients is a hard task computationally. There are algorithms that find the solution iteratively. However, finding the global optimum is not guaranteed with those algorithms. There are, on the other hand, simpler algorithms for finding the filter coefficients. These algorithms are computationally efficient but the statistical accuracy may be poor in some situations. In this section, we briefly describe one of the latter algorithms known as the *modified Yule-Walker* (MYW) method.

The MYW method consists of two stages. In the first stage, the AR parameters $\{a_i\}_{i=1}^{n}$ are

computed using (5). More precisely, writing (5) for $k = m+1, m+2, \ldots, m+M$, ($M$ to be defined later) in the matrix form and replacing the true covariances $\{r(k)\}$ by their corresponding sample estimates $\{\hat{r}(k)\}$ we get

$$\begin{bmatrix} \hat{r}(m) & \hat{r}(m-1) & \ldots & \hat{r}(m+1-n) \\ \hat{r}(m+1) & \hat{r}(m) & \ldots & \hat{r}(m+2-n) \\ \vdots & \vdots & \ddots & \vdots \\ \hat{r}(m+M-1) & \ldots & & \hat{r}(m+M-n) \end{bmatrix} \begin{bmatrix} \hat{a}_1 \\ \vdots \\ \hat{a}_n \end{bmatrix} = - \begin{bmatrix} \hat{r}(m+1) \\ \hat{r}(m+2) \\ \vdots \\ \hat{r}(m+M) \end{bmatrix}. \tag{20}$$

In order to solve this equation, we need M to be at least n. If we set $M = n$ in (20) we get

$$\begin{bmatrix} \hat{r}(m) & \ldots & \hat{r}(m-n+1) \\ \vdots & \ddots & \vdots \\ \hat{r}(m+n-1) & \ldots & \hat{r}(m) \end{bmatrix} \begin{bmatrix} \hat{a}_1 \\ \vdots \\ \hat{a}_n \end{bmatrix} = - \begin{bmatrix} \hat{r}(m+1) \\ \vdots \\ \hat{r}(m+n) \end{bmatrix}. \tag{21}$$

This equation is known as the MYW system of equations. The square matrix in (21) has been shown to be non-singular under mild conditions and hence the solution exists.

If we choose $M > n$ in (20), we will get an overdetermined system of equations. Since we replace the true covariances with the corresponding sample estimates, the resulting overdetermined system of equations does not necessarily have a solution. However, we can solve for AR parameters by using for instance the least square or total least square methods. We leave the discussion about whether increasing M helps the accuracy of AR estimates to the readers.

Once the MYW estimates of AR parameters $\{\hat{a}_i\}$ are found, we move to the next stage which is finding the spectra of the MA part. Using the MA model in (18), the spectra of the MA part can be written as

$$\sigma^2 |B(\omega)|^2 = \sum_{k=-m}^{m} \gamma_k e^{-i\omega k}$$

where

$$\gamma_k = E\Big\{ \big[B(q)e(t)\big] \big[B(q)e^*(t-k)\big] \Big\}$$

denotes the covariance of the MA part (q represents the shift operator; i.e. $q^k y(t) = y(t-k)$).

Now using the ARMA model, we have

$$A(q)y(t) = B(q)e(t)$$

and hence

$$\gamma_k = E\Big\{ \big[A(g)y(t)\big]\big[A(q)y^*(t-k)\big] \Big\} = \sum_{\ell=0}^{n}\sum_{p=0}^{n} a_\ell a_p^* E\big\{y(t-\ell)y^*(t-k-p)\big\}$$

$$= \sum_{\ell=0}^{n}\sum_{p=0}^{n} a_\ell a_p^* r(k+p-\ell), \qquad (a_0 = 1) \tag{22}$$

for $k = 0, \ldots, m$. Now inserting the estimated MYW parameters and estimated sample covariances, we get the following estimator of $\{\gamma_k\}$:

$$\hat{\gamma}_k = \sum_{\ell=0}^{n}\sum_{p=0}^{n} \hat{a}_\ell \hat{a}_p^* \hat{r}(k+p-\ell), \qquad \text{for} \quad k = 0, \ldots, m. \tag{23}$$

For $k = -1, \ldots, -m$, we assume that $\hat{\gamma}_k = \hat{\gamma}_{-k}^*$. Finally, the MYW spectrum is estimated by

$$\hat{\phi}(\omega) = \frac{\sum_{k=-m}^{m} \hat{\gamma}_k e^{-i\omega k}}{|\hat{A}(\omega)|^2} \tag{24}$$

with

$$\hat{A}(\omega) = 1 + \hat{a}_1 e^{-i\omega} + \ldots + \hat{a}_n e^{-in\omega}.$$

VII. Comparison of Different Estimators via an Example

In this section, we examine the properties of non-parametric spectral estimators for a broadband ARMA(4,4) signal with

$$A(q) = 1 - 1.3817q^{-1} + 1.5632q^{-2} - 0.8843q^{-3} + 0.4096q^{-4},$$

$$B(q) = 1 + 0.3544q^{-1} + 0.3508q^{-2} + 0.1736q^{-3} + 0.2401q^{-4},$$

and $\sigma^2 = 1$.

The pole-zero diagram of the system is depicted in Fig. 1 and the corresponding power spectral density is illustrated in Fig. 2.

We assume that $N = 512$ realizations of the ARMA signal are observed, which are then used to estimate sample covariance estimates required for different spectral estimators. We will use

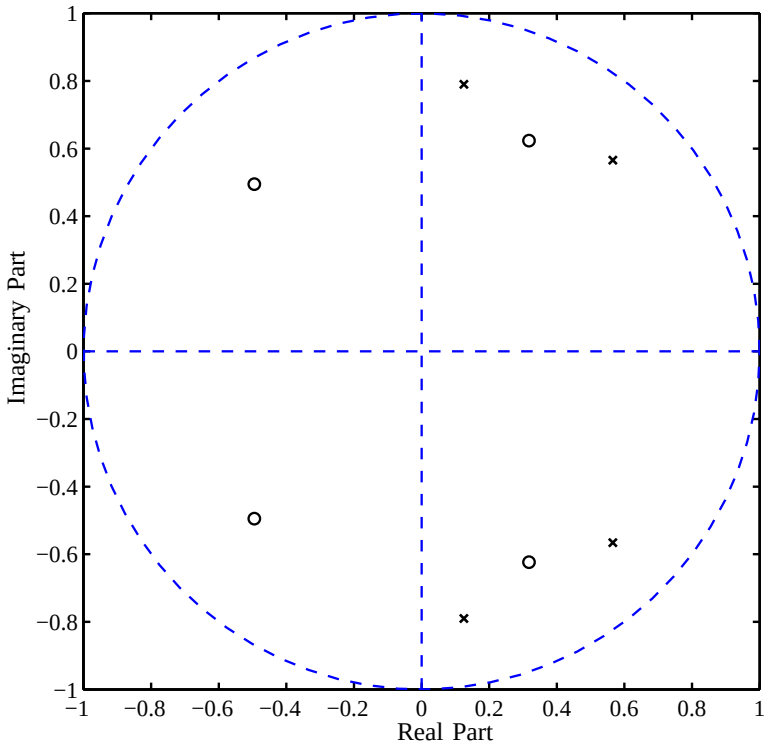

Fig. 1. Pole-zero diagram of the given ARMA signal.

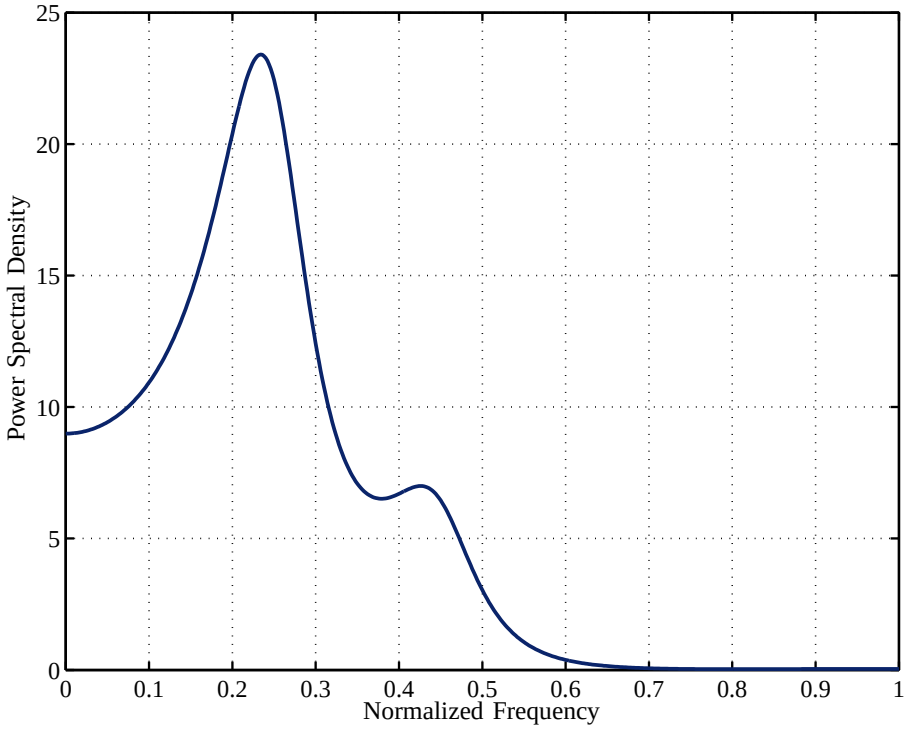

Fig. 2. Power spectral density of the given ARMA signal.

AR(4), AR(8), ARMA(4,4) and ARMA(8,8) methods. For the MYW method, we will use both $M = n$ and $M = 2n$.

Fig. 3 and 4 illustrate the estimated pole-zero diagram and the estimated power spectral density for the AR estimator with degree 4, for 10 overlaid estimation samples. Fig. 5 and 6 illustrate the same plots as Fig. 3 and 4 but for AR model with degree 8. As the result show by increasing the degree a better performance can be achieved. This is expected since the model with higher degree can predict the spectrum better.

Fig. 7 and 8 illustrate the estimated pole-zero diagram and the estimated power spectral density for the ARMA estimator with degrees $n = 4$, $m = 4$ and $M = n$, for 10 overlaid estimation samples. Fig. 9 and 10 illustrate the same plots as Fig. 7 and 8 but for the case with $M = 2n$.

Fig. 11 and 12 illustrate the estimated pole-zero diagram and the estimated power spectral density for the ARMA estimator with degrees $n = 8$, $m = 8$ and $M = n$, for 10 overlaid estimation samples. Fig. 13 and 14 illustrate the same plots as Fig. 11 and 12 but for the case with $M = 2n$.

To see the asymptotic behavior of the above schemes, we let the observed sequence to grow arbitrarily large ($N = 2^{15}$ for the illustration) and we compare different spectral estimation techniques. Fig. 15 and 16 illustrate the estimated pole-zero diagram and power spectral density for 10 overlaid estimation samples using AR(4) signal model. Fig. 17 and 18 illustrate the same but for AR(8) model.

Fig. 19 and 20 illustrate the asymptotic behavior of ARMA(4,4) method.

Finally, Fig. 21 illustrates the power spectral density estimates using periodogram method. The plot is obtained by averaging over 30 estimation samples.

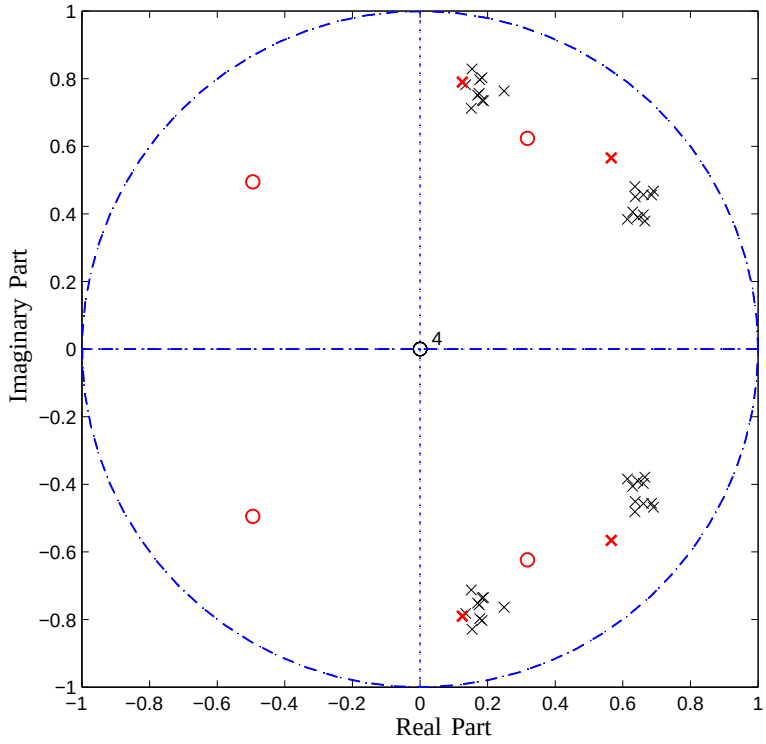

Fig. 3. Pole-zero diagram for 10 overlaid estimations using AR(4) method.

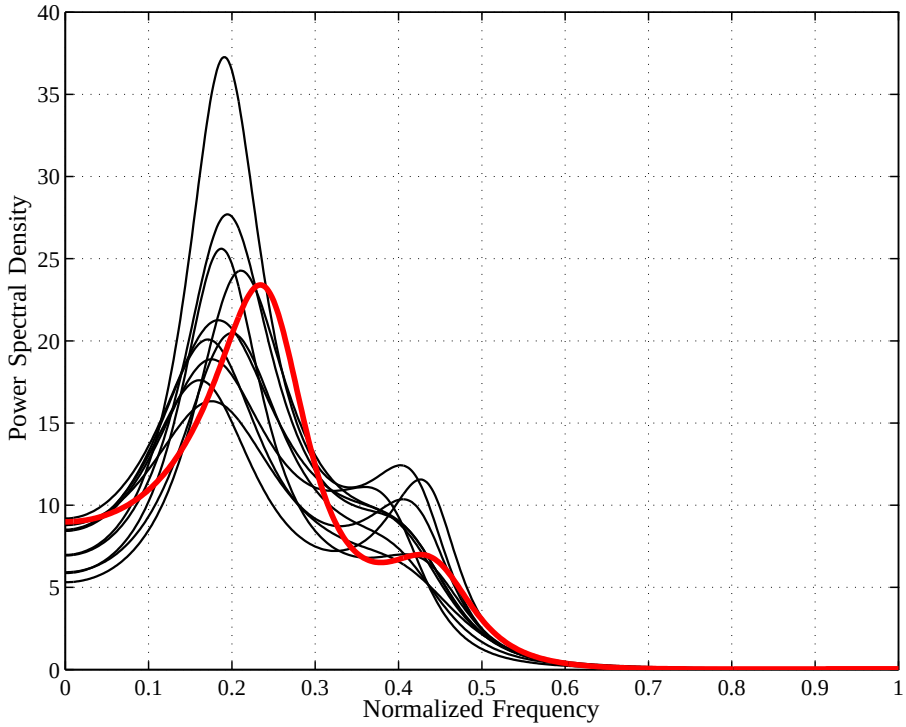

Fig. 4. Power spectral density estimates for 10 overlaid samples using AR(4) method.

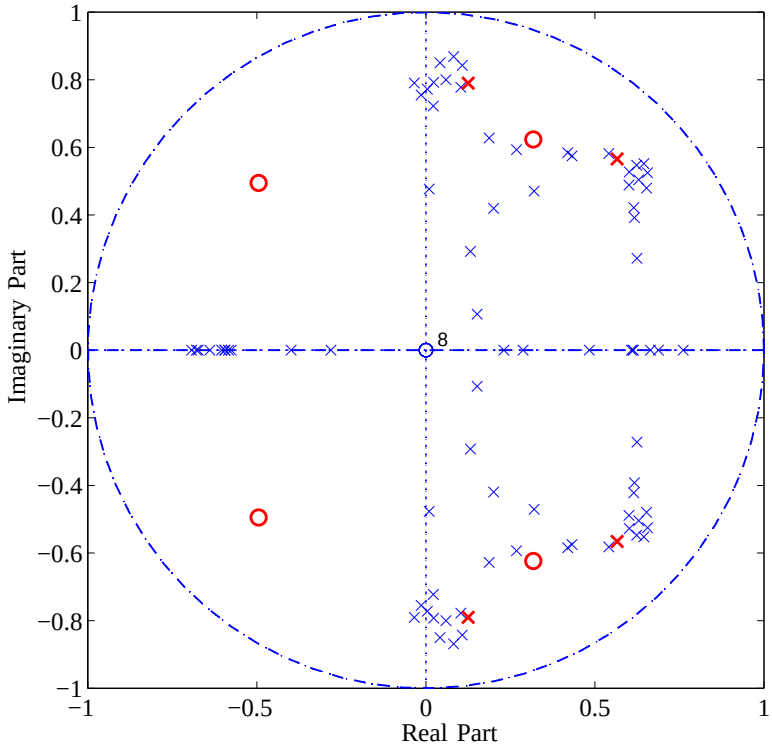

Fig. 5. Pole-zero diagram for 10 overlaid estimations using AR(8) method.

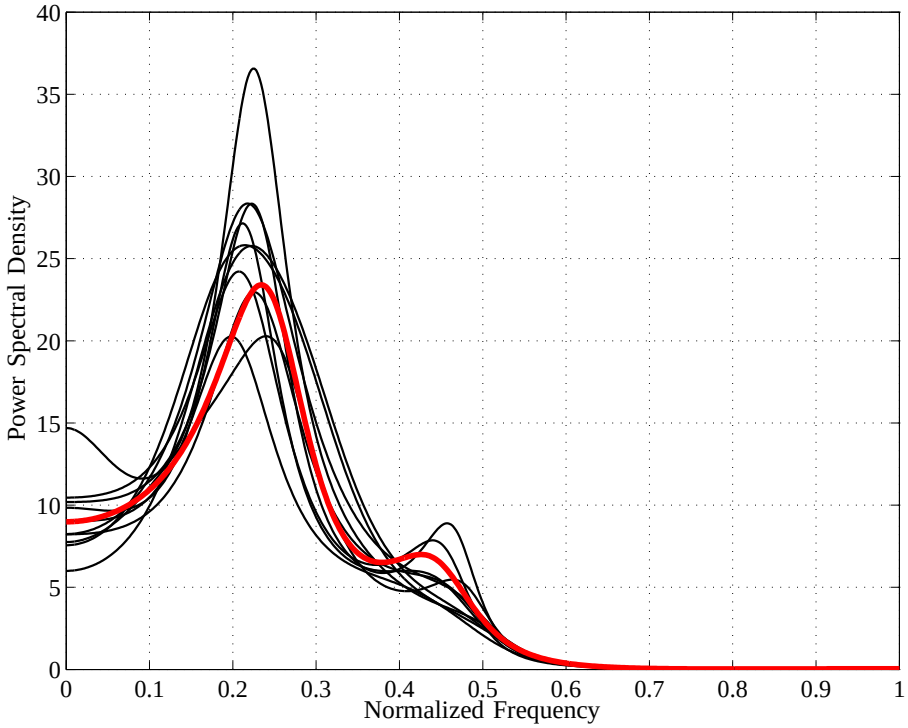

Fig. 6. Power spectral density estimates for 10 overlaid samples using AR(8) method.

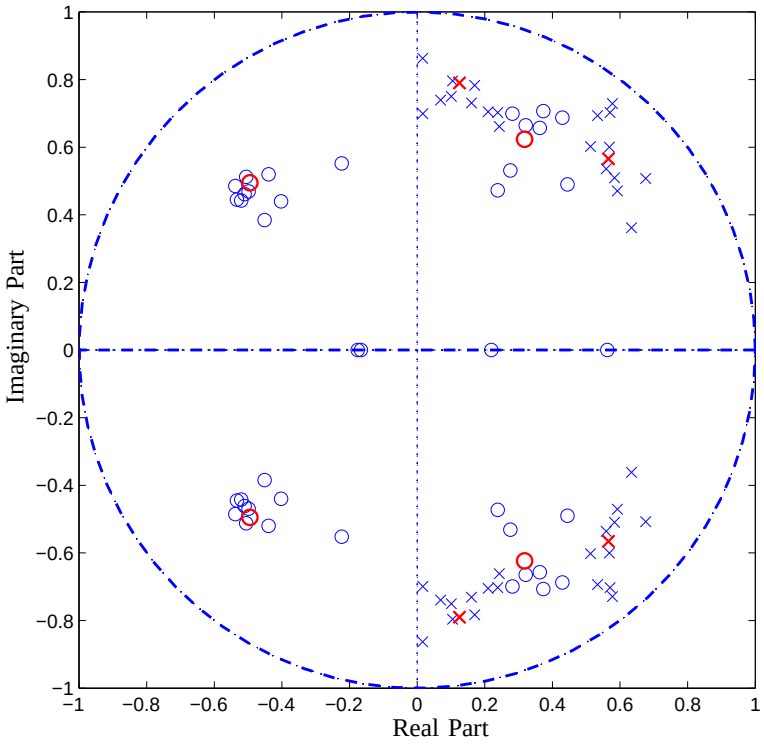

Fig. 7. Pole-zero diagram for 10 overlaid estimations using ARMA(4,4) method with $M = n$.

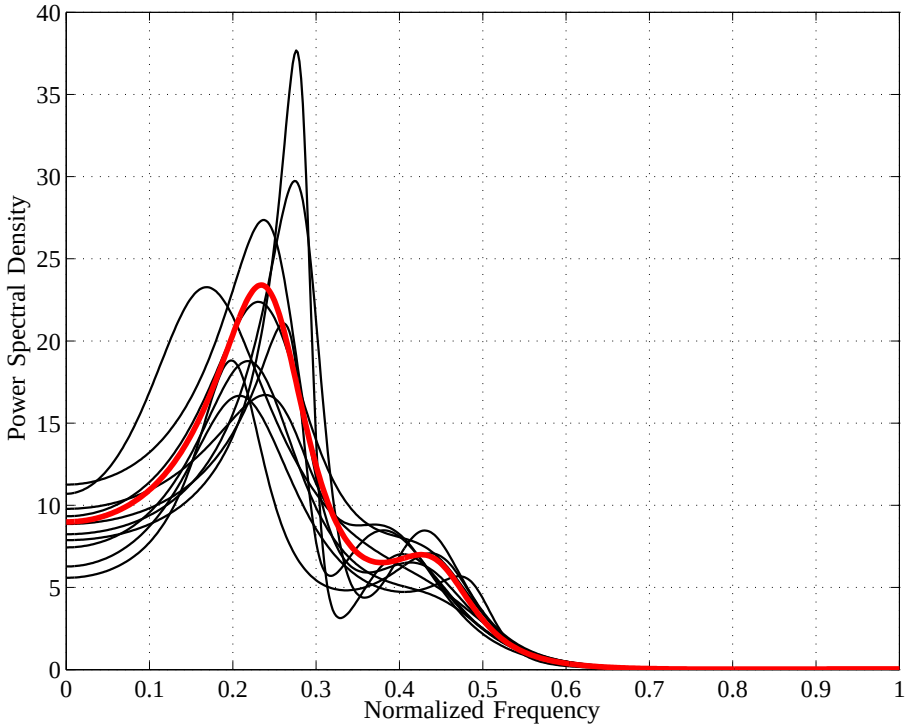

Fig. 8. Power spectral density estimates for 10 overlaid samples using ARMA(4,4) method with $M = n$.

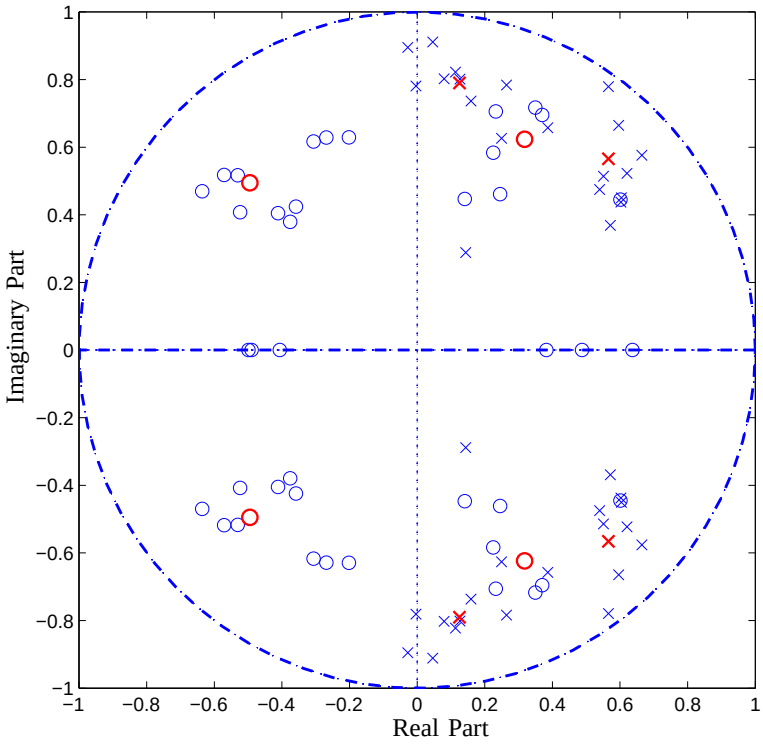

Fig. 9. Pole-zero diagram for 10 overlaid estimations using ARMA(4,4) method with $M = 2n$.

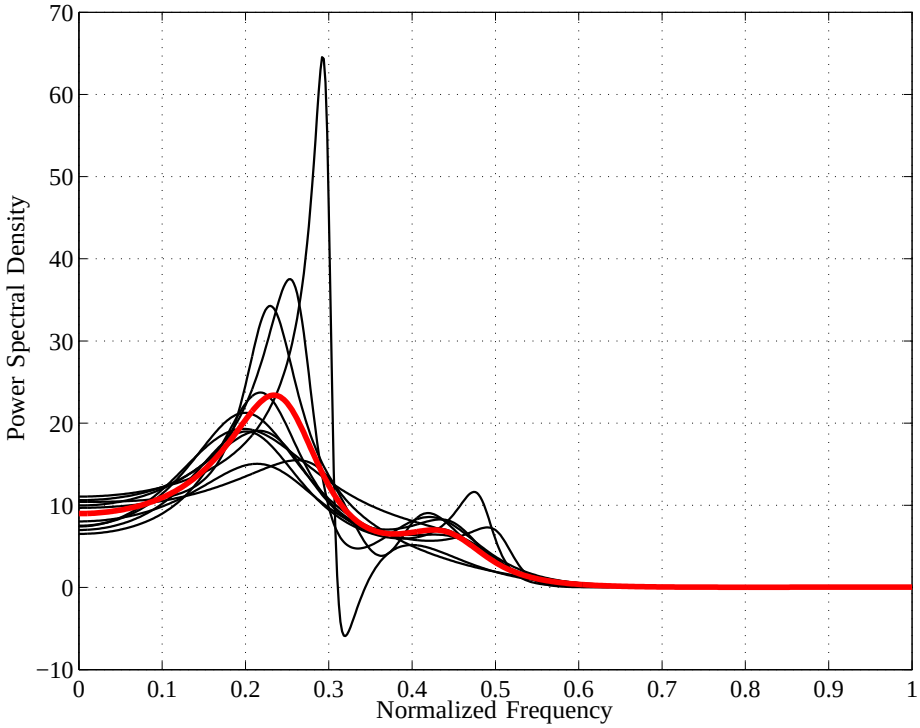

Fig. 10. Power spectral density estimates for 10 overlaid samples using ARMA(4,4) method with $M = 2n$.

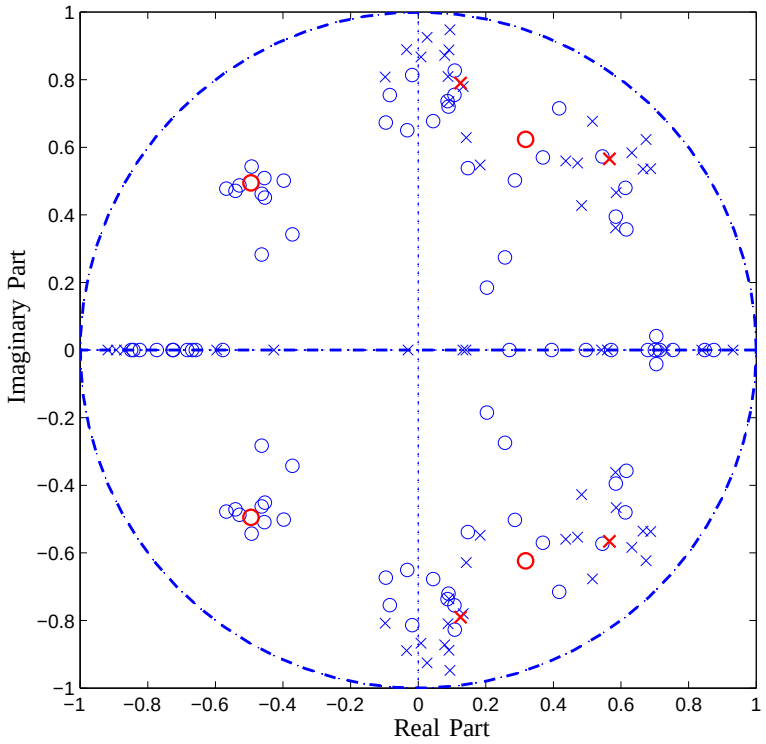

Fig. 11. Pole-zero diagram for 10 overlaid estimations using ARMA(8,8) method with $M = n$.

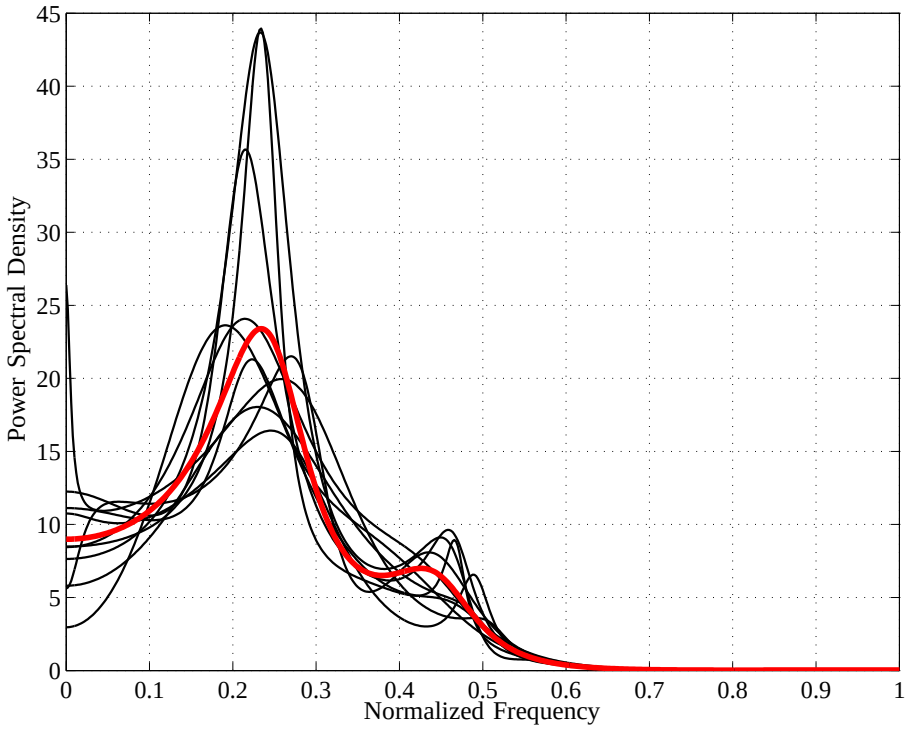

Fig. 12. Power spectral density estimates for 10 overlaid samples using ARMA(8,8) method with $M = n$.

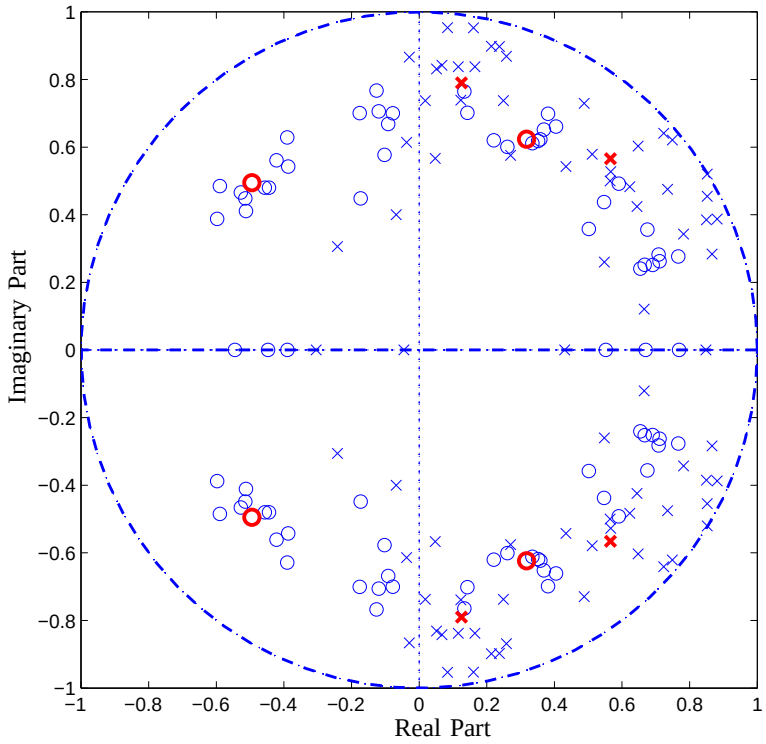

Fig. 13. Pole-zero diagram for 10 overlaid estimations using ARMA(8,8) method with $M = 2n$.

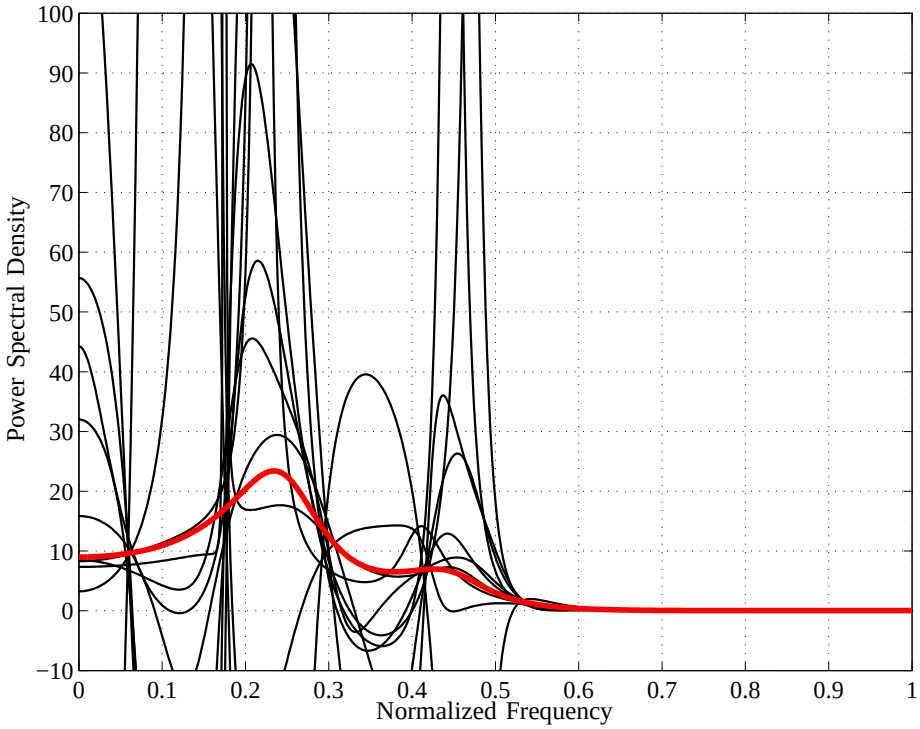

Fig. 14. Power spectral density estimates for 10 overlaid samples using ARMA(8,8) method with $M = 2n$.

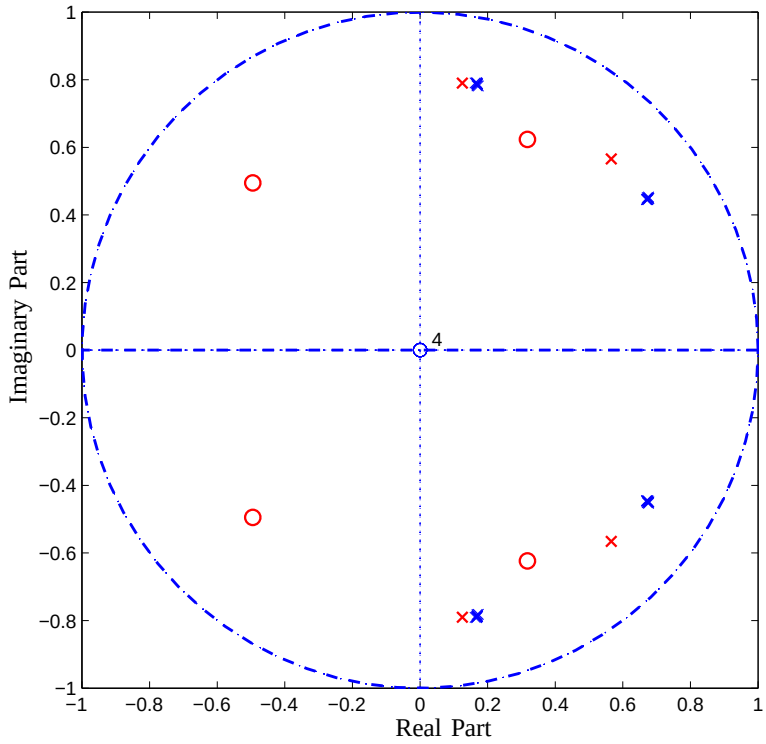

Fig. 15. Pole-zero diagram for 10 overlaid estimations using AR(4) method with many observations.

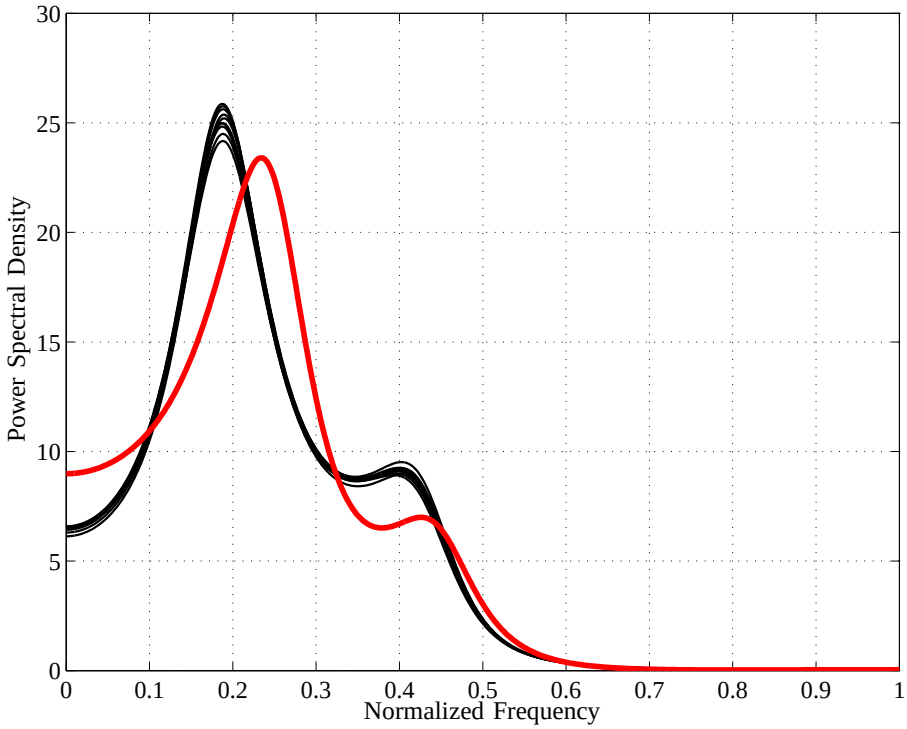

Fig. 16. Power spectral density estimates for 10 overlaid samples using AR(4) method with many observation.

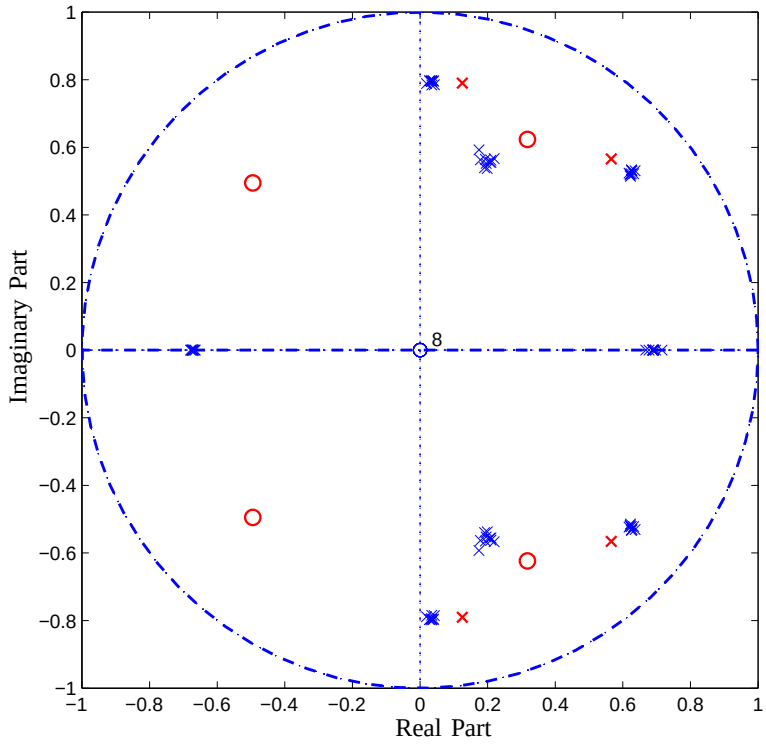

Fig. 17. Pole-zero diagram for 10 overlaid estimations using AR(8) method with many observations.

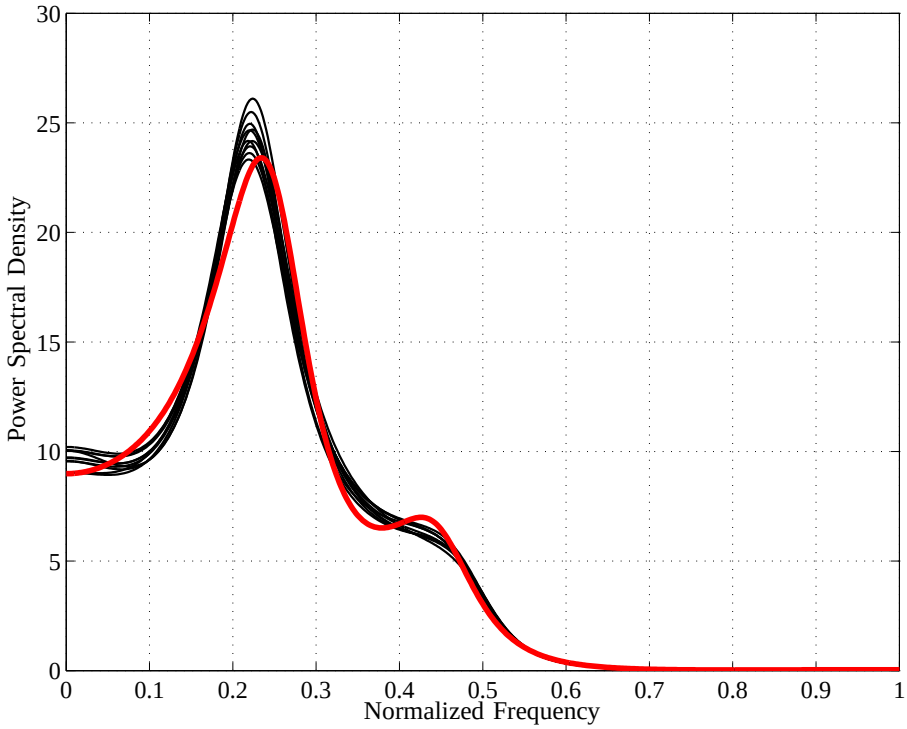

Fig. 18. Power spectral density estimates for 10 overlaid samples using AR(8) method with many observation.

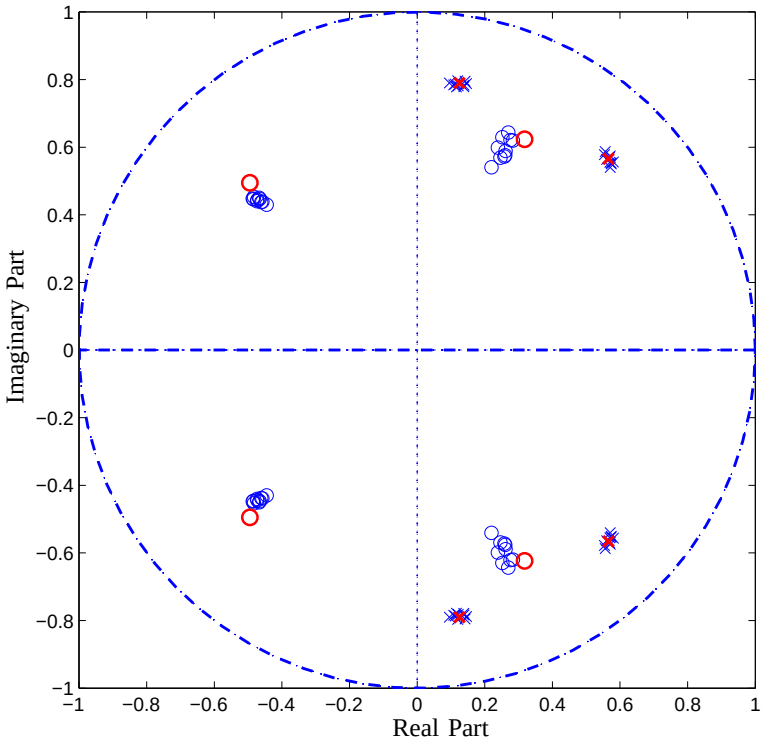

Fig. 19. Pole-zero diagram for 10 overlaid estimations using ARMA(4,4) method with many observations.

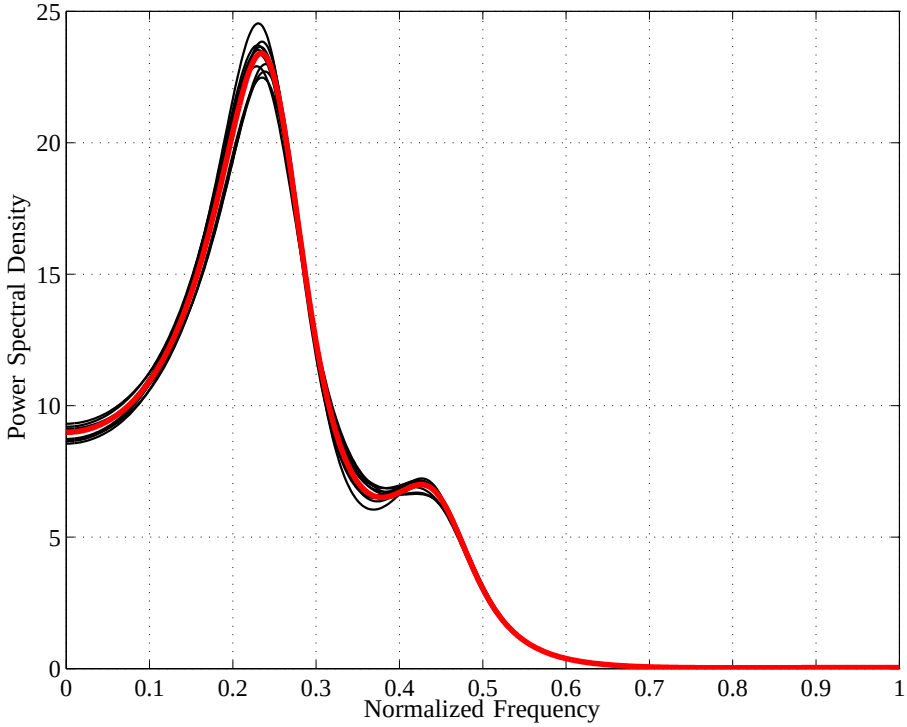

Fig. 20. Power spectral density estimates for 10 overlaid samples using ARMA(4,4) method with many observation.

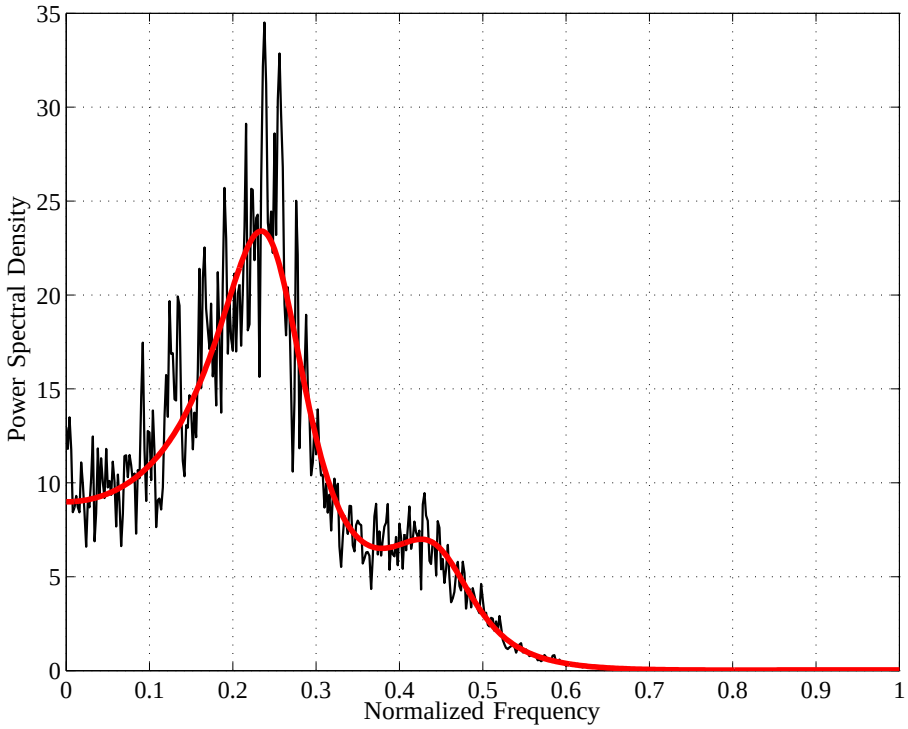

Fig. 21. Power spectral density estimates using periodogram method. The results are averaged over 30 estimation instances.